Eur Phys J C **37**, s1, s9–s26 (2004)
Digital Object Identifier (DOI) 10.1140/epjcd/s2004-01-002-1

EPJ C direct
electronic only

Charmonium at finite temperature in quenched lattice QCD

Takashi Umeda[1a], Kouji Nomura[2], and Hideo Matsufuru[3b]

[1] Center for Computational Physics, University of Tsukuba, Tsukuba 305-8577, Japan
[2] Department of Physics, Hiroshima University, Higashi-hiroshima 739-8526, Japan
[3] Yukawa Institute for Theoretical Physics, Kyoto University, Kyoto 606-8502, Japan

Received: 18 April 2003 / Accepted: 20 August 2003 /
Published Online: 18 February 2004 –

Abstract. We study charmonium correlators in pseudoscalar and vector channels at finite temperature using lattice QCD simulation in the quenched approximation. Anisotropic lattices are used in order to have sufficient numbers of degrees of freedom in the Euclidean temporal direction. We focus on the low energy structure of the spectral function, corresponding to the ground state in the hadron phase, by applying the smearing technique to enhance the contribution to the correlator from this region. We employ two analysis procedures: the maximum entropy method (MEM) for the extraction of the spectral function without assuming a specific form, to estimate the shape of the spectral function, and the standard χ^2 fit analysis using typical forms in accordance with the result of MEM, for a more quantitative evaluation. To verify the applicability of the procedures, we first analyze the smeared correlators as well as the point correlators at zero temperature. We find that by shortening the t-interval used for the analysis (a situation inevitable at $T > 0$) the reliability of MEM for point correlators is lost, while it subsists for smeared correlators. Then the smeared correlators at $T \simeq 0.9T_c$ and $1.1T_c$ are analyzed. At $T \simeq 0.9T_c$, the spectral function exhibits a strong peak, well approximated by a delta function corresponding to the ground state with almost the same mass as at $T = 0$. At $T \simeq 1.1T_c$, we find that the strong peak structure still persists at almost the same place as below T_c, but with a finite width of a few hundred MeV. This result indicates that the correlators possess a nontrivial structure even in the deconfined phase.

1 Introduction

The charmonium systems have been payed much attention as a signal of the QCD phase transition. Due to a change of the interquark potential by thermal effects, the J/ψ mass is expected to decrease when approaching the phase transition [1]. Above T_c, the screening of the interquark potential may dissolve the charmonium states, and the resulting J/ψ suppression has been regarded as one of the most important signals for detecting the formation of the plasma state [2,3,4].

In principle, lattice QCD simulations can provide information on such excitation modes based on a nonperturbative and model independent framework, since the correlation functions in the Euclidean temporal direction measured on a lattice are related to the real time retarded and advanced Green functions by analytic continuation from a single spectral function [5,6]. In practice, however, the extraction of reliable information from numerical data for correlators becomes increasingly difficult as the temperature increases. There are two restrictions on the correlators at finite temperature: the numbers of available degrees of freedom, and the physical extent in the temporal direction. The former can be improved by the use of anisotropic lattices, on which the temporal lattice spacings are finer than the spatial ones [6,7,8]. The latter restriction is, however, physically inevitable and may spoil standard procedures applicable at zero temperature.

Recently, there has been technical progress in the direct extraction of the spectral function from lattice data of correlators [9,10]. The key role is played by the maximum entropy method (MEM), combined with the singular value decomposition for constructing the functional bases in the space of spectral functions. At zero temperature this technique has reproduced spectra consistent with the standard fit analyses [9,11,12,13,14]. Application to systems at finite temperature is, however, not straightforward because of the two restrictions mentioned above [15]. In particular, shortness of temporal extent, $1/T$, makes it difficult to extract the correct low energy structure of the spectral function. Therefore, one at least needs to verify at $T = 0$ that the method produces results which are stable against variation of the t-interval. There have already been a number of applications of MEM for finite temperature [16,17,18,19], but as long as such tests are not systematically

[a] *Present address:* Yukawa Institute for Theoretical Physics, Kyoto University, Kyoto 606-8502, Japan
[b] *Present address:* Computing Research Center, High Energy Accelerator Research Organization (KEK), Ibaraki 305-0801, Japan

performed these results may contain uncontrolled uncertainties. In fact, we will show in this paper that MEM applied to point-point correlators at $T = 0$ with shortened t-interval fails to produce the correct spectral functions. We therefore apply the smearing technique to enhance the contribution of the low energy part to the correlators [12, 7,8]. For the smeared correlators at $T = 0$, MEM works, at least qualitatively, also with a shorter t-interval.

In this paper, charmonium correlators are investigated using lattice QCD simulations in the quenched approximation. We focus on properties of the ground state, more generally the low energy structure of the correlator, rather than the whole spectral function. This paper mainly deals with the following two subjects:

(1) A technical investigation of procedures for extraction of reliable information from the numerical data of correlators in the temporal direction. In addition to MEM, we apply the standard χ^2 fit analysis assuming a peak structure for the spectral function [20]. The latter approach complements the former, since MEM with small numbers of data points appears not work beyond the level of qualitative estimate for the shape of spectral function.

(2) A study of temperature effects on the correlators near to the deconfining phase transition. Below T_c, the question is whether the charmonium mass shifts, as expected from the potential model approach [1]. Above T_c, previous studies have indicated that nontrivial structures may survive [7,8]. The possibility of the existence of collective modes in the plasma phase is therefore carefully examined.

We use quenched anisotropic lattices with the renormalized anisotropy $\xi = a_\sigma/a_\tau = 4$ and the spatial lattice cutoff $a_\sigma^{-1} \simeq 2$ GeV. The phase transition occurs near $N_t = 28$, and hence sufficiently many points are available in the vicinity of T_c. At $T \simeq 0$ we try to determine the conditions for a reliable extraction of the spectral function. We find that for the point correlators, reliability of MEM with less than 24 t-points (meaning a physical t-range of less than $O(0.5\text{fm}) \sim 0.7T_c$) is not guaranteed with the present level of statistics. Therefore only the smeared correlators are analyzed at finite temperature, $T \simeq 0.9T_c$ and 1.1 T_c.

Here we comment on the smearing technique. Although the correlator of spatially extended operators has no direct relation to the physically observable dilepton production rate, the properties of collective excitations such as mass and width are unchanged and can be probed more efficiently. To the extent that these excitations drive the dilepton rate we can at least say something about their position and shape, if not about their strength. A disadvantage is the possibility of detecting a fake peak, which may be produced by the smearing even in the case of free quarks [16]. To distinguish such an artifact from a genuine physical peak we use besides the smearing function based on the wave function obtained at $T = 0$ also a narrower one of essentially half-width. We speak thereby of "smeared" and of "half-smeared" correlators (because the energy region enhanced by this narrower smearing function is wider, while the high frequency part of $O(1/a_\tau)$ is still sufficiently suppressed). Comparing the results of these two types of smeared correlators, one can argue whether the observed peak structure is an artifact of free quarks or physical indication of a collective mode.

This paper is organized as follows. In Sect. 2, we recall some fundamental properties of the spectral function. For later uses in the χ^2 fit analysis, presumable forms of the spectral function for a collective mode are discussed. Section 3 reviews anisotropic lattice actions and describes the parameters used in this paper. We also show the spectral function of the correlator of a free quark-antiquark pair, for comparison with the correlators from the Monte Carlo simulation. In Sect. 4 our analysis procedures are explained. Section 5 describes the setup of Monte Carlo simulation. The following three sections show the result of the numerical simulation. In Sect. 6 we analyze the correlators at zero temperature, as a preparation for the more involved situations at finite temperatures. Sections 7 and 8 show the results at $T \simeq 0.9T_c$ and $1.1T_c$, respectively. In each case, we first estimate the presumable form of the spectral function with MEM, and then apply the χ^2 fit analysis for a more quantitative evaluation of its structure. Section 9 is devoted to our conclusions on the technical and physical implications of the results. Our preliminary results have been reported in [21].

2 Spectral function

In this section β represents the inverse temperature and should not be confused with the coupling of gauge field which appears in later sections. For a finite lattice of temporal extent N_τ we have $\beta = 1/T = N_t a_\tau$. The Euclidean time is represented by τ in this section to make clear the distinction between the Euclidean and Minkowski formulations. In later sections we use also t as the Euclidean time, because no confusion is expected for the lattice QCD formulated in the Euclidean space.

We consider correlators of the form:

$$C(\tau) = \sum_{\mathbf{x}} \langle O(\mathbf{x},\tau) O^\dagger(0,0)\rangle, \tag{1}$$

where the operator $O(\mathbf{x},\tau)$ is a quark bilinear,

$$O(\mathbf{x},\tau) = \sum_{\mathbf{y}} \phi(\mathbf{y}) \bar{q}(\mathbf{x}+\mathbf{y},\tau) \Gamma q(\mathbf{x},\tau). \tag{2}$$

4×4 matrix Γ specifies the quantum number, such as, for example, $\Gamma = \gamma_5$ for pseudoscalar and γ_i $(i = 1,2,3)$ for vector channels. $\phi(\mathbf{y})$ is a smearing function defining the spatial extension of the bilinear operator. Since the smearing in general violates the gauge invariance of the correlator, one needs to fix the gauge or employ a gauge invariant form of the smearing function. We fix the configurations to the Coulomb gauge, since it is widely used and allows easy implementation of the smearing function. Source and sink operators are always identical in this work.

Point correlators correspond to a ultra local "smearing function" $\phi(\mathbf{y}) = \delta_{\mathbf{y},0}$ in (2). For the *smeared* correlators

we use smearing function of the form

$$\phi(\mathbf{y}) = \exp(-a|\mathbf{y}|^p), \tag{3}$$

where the parameters a and p are determined by fitting the wave function measured in the numerical simulation to the above form. The smearing technique described here was already applied to the problems of the charmonium correlators at $T > 0$ [8], as well as to the light meson correlators [7].

For a while let us consider the continuum Euclidean space. The Matsubara Green function is represented in terms of the spectral function as

$$G(\nu_n, \mathbf{p}) = \int_{-\infty}^{\infty} \frac{d\omega}{2\pi} \frac{\rho(\omega, \mathbf{p})}{i\nu_n - \omega + i\epsilon}. \tag{4}$$

The spectral function $\rho(\omega, \mathbf{p})$ is represented as

$$\rho(\omega, \mathbf{p}) = \frac{1}{2Z(\beta)} \sum_{n,m} (e^{-\beta E_n} - e^{-\beta E_m}) |\langle n|O(0)|m\rangle|^2 \times (2\pi)^4 \delta(\omega - E_m + E_n) \delta(\mathbf{p} - \mathbf{P}_m + \mathbf{P}_n), \tag{5}$$

which is an odd real function due to the bosonic nature of the present correlator and positive for $\omega > 0$.

The retarded and advanced Green functions for real time are represented as

$$G^R(\nu, \mathbf{p}) = \int_{-\infty}^{\infty} \frac{d\omega}{2\pi} \frac{\rho(\omega, \mathbf{p})}{\nu - \omega + i\epsilon} \tag{6}$$

$$G^A(\nu, \mathbf{p}) = \int_{-\infty}^{\infty} \frac{d\omega}{2\pi} \frac{\rho(\omega, \mathbf{p})}{\nu - \omega - i\epsilon} \tag{7}$$

with the same spectral function, $\rho(\omega, \mathbf{p})$ [5]. The spectral function is then represented as

$$\rho(\nu, \mathbf{p}) = -2\ \mathrm{Im} G^R(\nu, \mathbf{p}) = 2\ \mathrm{Im} G^A(\nu, \mathbf{p}). \tag{8}$$

Strictly speaking, the above integrations do not always converge, and one needs appropriate subtraction terms. On the other hand, the high frequency part of the spectral function is not practically significant in the numerical analysis, because of the strong suppression by $K(\tau, \omega)$ defined below, and of the existence of the lattice cutoff. We therefore do not consider these subtractions in this paper. We note that the smearing of the operator in (2) is performed only in the spatial directions, and therefore the analytic continuation of the Matsubara Green function to the real time Green functions is independent of this operation (but, of course, the spectral function depends on the operators, hence on smearing).

In the following we are only concerned with the correlators projected on the zero momentum states and discard the argument $\mathbf{p}$. Since the spectral function $\rho(\omega)$ is an odd function in ω, the correlator (1) is represented as

$$C(\tau) = \int_0^{\infty} \frac{d\omega}{2\pi} K(\tau, \omega) \rho(\omega). \tag{9}$$

where

$$K(\tau, \omega) = \frac{e^{-\omega\tau} + e^{-\beta\omega + \omega\tau}}{1 - e^{-\beta\omega}}. \tag{10}$$

In the numerical simulation of lattice QCD one measures the left hand side of (9). The question is how to solve the inverse problem to obtain $\rho(\omega)$ with limited data for $C(\tau)$. The procedures to extract information about $\rho(\omega)$ are described in Sect. 4.

Now we shall present several *ansätze* for the spectral function which will be used for later analysis of the lattice data, and discuss their physical implications. A simple representation of a collective mode is the following form of the retarded Green function:

$$G^R(\nu) = \frac{R(\nu)}{\nu - \mu + i\gamma(\nu)/2}, \tag{11}$$

where μ and $\gamma(\nu)$ express the dispersion and the width of the mode. The corresponding spectral function is the well-known Breit-Wigner form. We shall neglect the frequency dependence of the width γ for simplicity. Taking the oddness of the bosonic spectral function into account, $\rho(\omega)$ reads

$$\rho(\omega) = \frac{\gamma R(\omega)}{(\omega - m)^2 + \gamma^2/4} - \frac{\gamma R(\omega)}{(\omega + m)^2 + \gamma^2/4}. \tag{12}$$

If the quantum numbers of the operators used to represent the collective mode are the correct ones, the physical properties associated with the mode, characterized by μ and γ, are independent of the particular operator. Therefore the smeared operators can be used to observe these quantities. However, the smearing does change the overlap of the operator with the state, $R(\omega)$. Therefore the effects depending on $R(\omega)$ and those coming only from the peak structure (represented with μ and γ) should be distinguished. If the change of $R(\omega)$ is sufficiently gentle over the region of the observed peak, the ω dependence in $R(\omega)$ is negligible.

Instead of (12), at zero temperature one often uses the relativistic Breit-Wigner type form:

$$\rho(\omega) = \frac{\mathrm{sign}(\omega)\omega^2 m\gamma(4R/m)}{(\omega^2 - m^2)^2 + m^2\gamma^2}. \tag{13}$$

This form shows a similar behavior to (12) around the peak position. However, the behavior far from the peak is different. In particular (12) and (13) give different contribution to the integral (9) near vanishing ω: In the vicinity of $\omega = 0$, (12) behaves linearly in ω, while (13) behaves linearly in ω^2. Since $K(\tau, \omega)$ behaves as $(2 - \beta\omega)/\beta\omega$, (12) gives a t-independent contribution to the integral (9) [15]. We note that there is no indication of linear behavior in ω in the small ω region of the spectral functions obtained from our numerical data with MEM, as shown in Sect. 7 and 8. Therefore, in the χ^2 fit analysis, we use the form of (13) as *ansatz* for the spectral function to which the lattice data are fitted. While the use of (13) is valid at zero temperature, it should only be taken as a representative form of peak structure at $T > 0$, and hence the parameters m and γ do not have a strict sense but represent only a convenient parameterization of the peak.

In the limit of $\gamma \to 0$, both (12) and (13) tend towards a delta function form,

$$\rho(\omega) = 2\pi R \left[\delta(\omega - m) - \delta(\omega + m)\right]. \tag{14}$$

This form corresponds to the standard exponential fit of correlators used in the hadron spectroscopy at zero temperature.

3 Anisotropic lattice QCD

3.1 Anisotropic lattice actions

For analysis of the correlators in the temporal direction at $T > 0$ the fine temporal resolution is very important to extract meaningful information [7,8,20]. Anisotropic lattices have become a powerful tool to achieve sufficiently high temporal cutoff while keeping total computational size modest. In the following, we summarize the anisotropic lattice actions employed in this work. The parameters we use are described in the next subsection.

For the gauge field, we adopt the standard Wilson plaquette action [22],

$$S_G = \beta\gamma_G \sum_x \sum_{i=1}^{3} \left[1 - \frac{1}{3}\mathrm{ReTr}U_{i4}(x)\right] + \frac{\beta}{\gamma_G} \sum_x \sum_{i<j=1}^{3} \left[1 - \frac{1}{3}\mathrm{ReTr}U_{ij}(x)\right], \quad (15)$$

where $U_{\mu\nu}$ is a product of link variables along a plaquette in the μ-ν plane. Here the parameters β and γ_G are bare coupling and bare anisotropy, respectively.

For the quark field we use the $O(a)$ improved Wilson-type action [8,23,24]:

$$S_q = \sum_{x,y} \bar{q}(x) K(x,y) q(y), \quad (16)$$

$$\begin{aligned} K(x,y) = \delta_{xy} & \\ -\kappa_\tau & \left[(1-\gamma_4)U_4(x)\delta_{x+\hat{4},y} + (1+\gamma_4)U_4(x-\hat{4})\delta_{x-\hat{4},y}\right] \\ -\kappa_\sigma & \sum_{i=1}^{3} \left[(r-\gamma_i)U_i(x)\delta_{x+\hat{i},y} + (r+\gamma_i)U_i(x-\hat{i})\delta_{x-\hat{i},y}\right] \\ & -\kappa_\sigma c_E \sum_{i=1}^{3} \sigma_{4i} F_{4i}(x)\delta_{x,y} \\ & -\kappa_\sigma c_B \sum_{i>j=1}^{3} \sigma_{ij} F_{ij}(x)\delta_{x,y}. \end{aligned} \quad (17)$$

where κ_σ and κ_τ are the spatial and temporal hopping parameters, respectively, r is the spatial Wilson parameter, and c_E, c_B are the clover coefficients for the $O(a)$ improvement. We set $r = 1/\xi$ and c_E, c_B to the tadpole-improved tree-level values, and vary the two parameters κ_σ and κ_τ to change the quark mass and the fermionic anisotropy. The tadpole improvement [25] is performed by rescaling the link variables as $U_i(x) \to U_i(x)/u_\sigma$ and $U_4(x) \to U_4(x)/u_\tau$, respectively, with the corresponding mean-field values of the spatial and temporal link variables, u_σ and u_τ. Then c_E and c_B with the choice $r = 1/\xi$ read as

$$c_E = 1/u_\sigma u_\tau^2, \qquad c_B = 1/u_\sigma^3. \quad (18)$$

Instead of $(\kappa_\sigma, \kappa_\tau)$, it is convenient to use the parameters

$$\gamma_F \equiv u_\tau\kappa_\tau / u_\sigma\kappa_\sigma, \quad (19)$$

$$\frac{1}{\kappa} \equiv \frac{1}{u_\sigma\kappa_\sigma} - 2(\gamma_F + 3r - 4) = 2(m_0\gamma_F + 4), \quad (20)$$

where m_0 is the bare quark mass in temporal lattice units. κ plays the same role as on isotropic lattices, and controls the bare quark mass. γ_F is the bare fermionic anisotropy.

The lattice quark field $q(x)$ in the action (17) is related to the dimensionful field $\psi(x)$ as

$$\psi(x) = a_\sigma^{-3/2} Z_q(\beta,\kappa)\mathcal{K}(\kappa) q(x), \quad (21)$$

where we assume $m_Q \ll a_\tau^{-1}$. $\mathcal{K}(\kappa)$ is so-called KLM normalization factor [26],

$$\begin{aligned} \mathcal{K}(\kappa) &= [2u_\tau\kappa_\tau(1+m_0)]^{1/2} \\ &= \left[\frac{1+2\kappa(\gamma_F-4)}{1+2\kappa(\gamma_F+3r-4)}\right]^{1/2}. \end{aligned} \quad (22)$$

We consider the tadpole-improved tree-level matching of the fields in continuum and lattice theories, and hence Z_q is set to unity.

3.2 Parameters

We here describe the parameters used in this paper. First, we discuss the calibration of gauge and quark fields. In an interacting theory, the renormalized anisotropy $\xi = a_\sigma/a_\tau$ generally differs from the bare anisotropy parameters γ_G and γ_F. Therefore one needs to tune the latter such that

$$\xi_G(\gamma_G,\gamma_F) = \xi_F(\gamma_G,\gamma_F) = \xi \quad (23)$$

holds, where ξ_G and ξ_F are the observed anisotropies defined through the gauge and fermionic observables, respectively. In quenched simulations, one can calibrate the gauge and fermion fields separately, first the former, and then the latter.

For the calibration of the gauge field, we refer to an elaborated work by Klassen [27] which uses Wilson loops in the spatial-spatial and spatial-temporal planes and is performed at 1% accuracy level. Making use of his relation of γ_G to β and ξ, we choose $\beta = 6.10$ and $\gamma_G = 3.2108$ corresponding to the renormalized anisotropy $\xi = 4$. These values were also adopted in [24], and correspond to the spatial lattice cutoff $a_\sigma^{-1} = 2.030(13)$ GeV set by the hadronic radius r_0 [28].

For the quark field, we use the result of [24] in which the calibration was performed on the same lattice as this work using the meson dispersion relation in a quark mass region including the charm quark mass. Accordingly, we adopt $\kappa = 0.112$ and $\gamma_F = 4.00$, namely $m_q = 0.121$, as

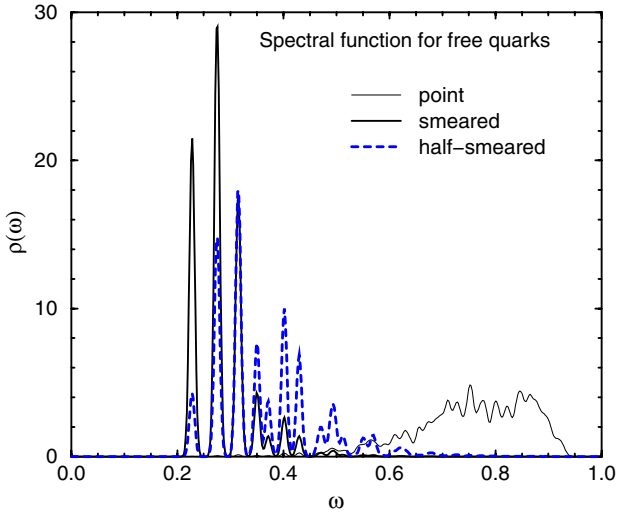

Fig. 1. The spectral functions for the pseudoscalar correlators composed of free quarks at $T = 0$

the values corresponding to the charm quark mass. (In [29] it was argued that the value of γ_F tuned for the massless quark is also applicable to the charm quark mass. For historical reason, however, we use the result of the mass dependent tuning in [24]. The difference is actually small and does not cause any significant effect.)

As smearing function we use the result for the wave function in the Coulomb gauge at $T = 0$. For the vector channel the fit to (3) yields $a = 0.2275(9)$ and $p = 1.258(5)$. These values are used for both the pseudoscalar and vector correlators.

In addition, we also use a narrower smearing function with $a = 0.45$ and the same p. The correlators smeared with this function are called *half-smeared* correlators, since the smearing function has about twice the slope as the main one and hence a smaller smearing effect is expected: the low energy part of the correlator is only partially enhanced, while the high energy part of $O(1/a_\tau)$ is sufficiently reduced. This intermediate smearing function plays an important role at $T > T_c$ in examining whether the observed peak structure of the spectral function for the smeared correlator is an artifact of smearing or a genuine physical effect (Sect. 8).

3.3 Free quark case

In [16] it was pointed out that the smearing may produce an artificial peak in a spectral function even for non-interacting quark and antiquark. In order to distinguish a genuine physical peak from such an artificial one, one needs to know how it looks like through the analysis applied when almost free quark picture is realized. For a comparison of the result of Monte Carlo simulation with the free quark case, the analysis of the latter should be performed under a condition as much similar to the former as possible. We therefore consider spectral functions of systems composed of free quarks with discretized momenta on a finite lattice of the same size as the simulation.

The spectral function of the correlator (1) in the case of free quarks is obtained from the expression (5). In the case of vanishing total momentum, for positive frequency,

$$\rho(\omega) = \frac{\pi}{Z}\sum_{\mathbf{p}}[1 - e^{-N_t 2E(\mathbf{p})}]\tilde{\phi}(\mathbf{p})^2 \times \sum_{j,k=1,2}\left[\frac{\bar{v}_j(-p)\Gamma u_k(p)}{2E(p)}\right]^2 \delta\left(\omega - 2E(\mathbf{p})\right) \quad (24)$$

where $u_j(p)$ and $v_j(p)$ are the quark and antiquark spinors with j-th spin, and $\tilde{\phi}(\mathbf{p})$ is the Fourier transform of $\phi(\mathbf{y})$. The summation in $\mathbf{p}$ is taken over all modes on the finite lattice of the same size as in Monte Carlo simulation, 20^3. With the present lattice quark action, the energy of free quark, $E(\mathbf{p})$, satisfies the dispersion relation [8,23]

$$\cosh E(\mathbf{p}) = 1 + \frac{\bar{\mathbf{p}}^2 + \left[m_0 + \frac{r}{2\gamma_F}\hat{\mathbf{p}}^2\right]^2}{2\left[1 + m_0 + \frac{r}{2\gamma_F}\hat{\mathbf{p}}^2\right]}, \quad (25)$$

where $\bar{p}_i = (1/\gamma_F)\sin p_i$ and $\hat{p}_i = 2\sin(p_i/2)$. We set the bare quark anisotropy $\gamma_F = \xi = 4$ and the bare quark mass $m_0 = 0.121$ such that the free quark has the same value as in the Monte Carlo simulation.

Figure 1 shows the spectral functions of point, smeared, and half-smeared correlators composed of free quarks in PS channel. The integral of these functions are normalized to unity. Since on the finite lattice the spectral function is a sum of delta functions, we represent each contribution at momentum $\mathbf{p}$ with a Gaussian of width 0.005 to make it visible in Fig. 1. As clearly shown in the figure, the smearing of the operator strongly enhances the low energy part of the spectral function, as compared to the point correlator. In the (fully) smeared correlator, several low momentum states over the range of ω about 0.1 dominate the correlator. From this correlator, therefore, an analysis with poor energy resolution in ω might produce a peak with full width of order of 0.1 instead of a sum of distinct peaks corresponding to individual momentum states. As we will see in Sect. 4.4, the χ^2 fit analysis with the single Breit-Wigner type *ansatz* applied to the smeared correlator composed of free quarks produces a much narrower peak with the width of about 0.027 centered at $\omega \simeq 0.275$. This is of the same order of magnitude as the width extracted from the correlators in Monte Carlo simulation at $T \simeq 1.1T_c$. Therefore this occasion must be examined carefully.

It is for this purpose that the half-smeared correlator is introduced. As shown in Fig. 1, a slightly higher and wider frequency region contributes dominantly to the half-smeared correlator than to the smeared one. If the correlator is approximated by a single peak, the peak will be centered at larger energy and have wider width as compared to those of the smeared correlator. This behavior is verified in Sect. 4 by applying the χ^2 fit analysis to the correlators composed of free quarks. Therefore, comparing the results for spectral functions for the smeared and half-smeared correlators can help judging whether the peak

observed from the simulation data is a genuine excitation mode or an artifact brought by the smearing.

Although we argued the case with almost free quarks with the correlators composed of contributions from discrete momentum modes, at nonzero coupling each momentum mode fluctuates and its contribution to the spectral function is smeared. In such a case, the spectral function may become smoother than as is shown in Fig. 1 (in Fig. 1 the Gaussian function is introduced by hand). Through analysis procedures, MEM and χ^2 fit, such a spectral function should be observed as a peak with larger width than the case without fluctuation. Therefore judging whether the observed peak is physical or artificial is rather easy, if the observed peak in Monte Carlo simulation has a small width. While such a judgment will become more difficult as the temperature increases, in present work the observed widths in numerical simulation are sufficiently small as shown in later sections.

4 Analysis procedure

4.1 Strategy of analysis

One of the goals of this work is to investigate techniques to extract the relevant information of the spectral function from the correlators with limited numbers of the degrees of freedom. We treat an inverse problem represented as

$$C(t) = \int_0^\infty d\omega K(t,\omega) A(\omega), \tag{26}$$

where $C(t)$ is the given lattice result for the correlator, and the spectral function $A(\omega)$ is what we need to obtain. Hereafter we shall denote the spectral function reconstructed from the lattice data $A(\omega)$ instead of $\rho(\omega)$ $(\times(2\pi)^{-1})$. Unless stated otherwise, the variables are in temporal lattice units in the following. The kernel $K(t,\omega)$ is given as

$$K(t,\omega) = \frac{e^{-\omega t} + e^{-\omega(N_t - t)}}{1 - e^{-N_t \omega}}. \tag{27}$$

This is the continuum type kernel, and an alternative form of the kernel which explicitly incorporate the lattice structure was also applied in the literatures [9,16]. We have seen no significant difference in applying the two kernels, therefore we shall not further discuss this point. In practice, the above integration over the frequency ω is replaced by a summation with sufficiently fine discretization $\Delta\omega$ and a cut off at some maximum value ω_{max}.

As already mentioned, one of the main analysis procedures is the maximum entropy method (MEM) [9]. Before applying it to finite temperature problems, one should verify its applicability under the condition which one encounters at $T > 0$. For this we test how the result changes when varying the number of data points used in analysis for the correlators at $T = 0$. The condition to be satisfied is that the ground state peak – which we know to exist at $T = 0$ – is correctly reproduced, at least at a qualitative level. We stress that without such verification, the result of MEM may contain uncontrolled artifacts at finite temperature. Concerning quantitative questions, we find that with reduced number of data points, MEM hardly gives a result beyond the qualitative level, for example for the width of a peak.

Another technique in our hand is the standard χ^2 fit assuming a certain *ansatz* for the spectral function. This method has been applied to a problem of glueballs at finite temperature [20]. A disadvantage of this approach is that one needs to assume a form of the spectral function, which introduces a bias. For this purpose, the result of MEM can be a good guide. Once a specific *ansatz* is used, the χ^2 fit gives much more reliable results than MEM for the parameters, both in statistical as well as systematic sense.

Therefore MEM and the χ^2 fit are complementary to each other at this stage of computational power, and in combination provide a more reliable way to analyze the structure of spectral functions than taken independently. We thus propose a two-step procedure: we first apply MEM to the correlators, for a rough estimate of the shape of spectral function. Once a presumable form is known, we then examine this form using χ^2 fit, and estimate the values of parameters such as the mass and width of a peak structure.

4.2 Maximum entropy method

Our MEM analysis basically follows [9], which reviews in detail the maximum entropy method applied to data of lattice QCD simulation. Here we briefly summarize just several formulae necessary for the later description of our analysis.

To obtain $A(\omega)$ from $C(t)$ by solving the inverse problem (26), the maximum entropy method maximizes a functional

$$Q(A;\alpha) = \alpha S[A] - L[A]. \tag{28}$$

$L[A]$ is the likelihood function,

$$L[A] = \frac{1}{2} \sum_{t_1,t_2} [C(t_i) - C_A(t_i)] V(t_i,t_j)^{-1} [C(t_j) - C_A(t_j)], \tag{29}$$

where $C_A(t)$ is the resulting correlator (26) for the trial $A(\omega)$, and $V(t_i,t_j)$ is the covariance matrix of the data

$$V(t_i,t_j) = \frac{1}{N(N-1)} \sum_{k=1}^{N} [C_k(t_i) - C(t_i)] [C_k(t_j) - C(t_j)] \tag{30}$$

with $C_k(t)$ the k-th sample of the correlator. The standard χ^2 fit minimizes this functional L. The Shannon-Jaynes entropy $S[A]$ is defined as

$$S[A] = \int_0^\infty d\omega \left[A(\omega) - m(\omega) - A(\omega) \log\left(\frac{A(\omega)}{m(\omega)} \right) \right]. \tag{31}$$

The function $m(\omega)$ is called the default model, and should be given as a plausible form of $A(\omega)$. The parameter α can

be integrated out at the last stage of calculation. Following [9], we use a form

$$m(\omega) = m_{DM}\omega^2. \tag{32}$$

In the case of point correlators, a natural choice of m_{DM} is determined according to the asymptotic behavior of the meson correlators at large ω in perturbation theory. Although such an asymptotic behavior is not observed in practical simulation because of the finite lattice cutoff, this form has been successfully applied to problems at zero temperature [9,13]. For the smeared correlators, the situation is more subtle, since the high frequency part of the correlator is suppressed by the smearing function. We therefore adopt a practical choice: we normalize the smeared correlator so as to produce the same overlap with the ground state as the point correlator. Then the same normalization is also applied to the correlators at finite temperatures, and we observe how the result changes with the change of m_{DM}.

In the maximization step of $Q(A;\alpha)$ the singular value decomposition of the kernel $K(t,\omega)$ is used. Then the spectral function is represented as a linear combination of the eigenfunctions of $K(t,\omega)$. The number of degrees of freedom of $A(\omega)$ is accordingly reduced to the number of data points of the correlator. Although the coefficients of the linear combination for $A(\omega)$ can in principle be determined uniquely from the data without introducing an entropy term, the small eigenvalues of $K(t,\omega)$, θ_i, lead for the spectral function to a singular behavior; hence truncation at some i is practically required [10]. In MEM, the addition of the entropy term stabilizes the problem and guarantees an unique solution for the coefficients of the eigenfunctions [9]. In our analysis, we use only the basis functions for which $\theta_i > 10^{-12} \times \theta_1$ holds, where θ_i is i-th largest singular value. This restriction has no significant effect on the result.

4.3 χ^2 fit with *ansatz* for the spectral function

The standard χ^2 fit method minimizes the likelihood function L, (29), with an assumed form for the spectral function. A most simple form for fit function is the delta function:

$$A_{pole}(\omega; r, m) = r\delta(\omega - m). \tag{33}$$

This form is referred to as *pole ansatz* in the following. At $T = 0$, a sum of several pole terms should describe well the correlators. For the correlators below T_c, where narrow thermal widths are expected, the multi-pole form is also convenient to test this assumption.

As noted in Sect. 2, to describe a peak structure with finite width we adopt the relativistic Breit-Wigner form (referred to as BW form),

$$A_{BW}(\omega; r, m, \gamma) = \frac{\omega^2 r m \gamma}{(\omega^2 - m^2)^2 + m^2\gamma^2}. \tag{34}$$

This is the same form as (13), with slightly modified notation for convenience. This *ansatz* neglects the ω dependence of r, and hence is valid only for the case that the width of the peak, γ, is sufficiently small compared with the change of the smearing function in the region of interest.

Combining these two forms, we fit the numerical data of correlators to the following *ansätze*:

2-pole form: this form is suitable for description of correlators at $T = 0$. It is also expected to be a good representation of correlators at $T < T_c$;

$$A(\omega) = A_{pole}(\omega; r_0, m_0) + A_{pole}(\omega; r_1, m_1). \tag{35}$$

1-BW form: if the contribution from the high frequency part of the spectral function is negligible, a collective excitation at low energy is expected to be well represented by a single Breit-Wigner type *ansatz*:

$$A(\omega) = A_{BW}(\omega; r_0, m_0, \gamma_0). \tag{36}$$

This form is also a good representation for the spectral function of the smeared correlator composed of free quarks.

BW+pole form: although the lowest peak is well represented with the Breit-Wigner type function, there may exist contribution from high frequency region. Since the smearing of operator suppress such contribution, remaining effects of this region may be represented as a single pole-like term. This is the reason that we fit the data to the form

$$A(\omega) = A_{BW}(\omega; r_0, m_0, \gamma_0) + A_{pole}(\omega; r_1, m_1). \tag{37}$$

This is the most general *ansatz* for χ^2 fit in this paper.

These *ansätze* forms are the basis for the analysis of the lowest peak structure, which corresponds to the ground state at $T < T_c$. The structure in the high frequency region is out of the scope of this paper.

4.4 Analysis of correlators composed of free quarks

To learn how to distinguish physical features of the correlators from artifacts due to the smearing we apply MEM and the χ^2 fit analyses to the correlators composed of free quarks on our lattice, which were discussed in Sect. 3.3.

For the MEM analysis, the fluctuations of the correlators are given by hand in the same manner as the mock data analyses in [9,13]. The deviations of the correlators are less than those of the data from the Monte Carlo simulation. Figure 2 shows the result of MEM applied to the smeared correlator in pseudoscalar channel composed of free quarks at $T = 0$. The upper bound of t region used for the analysis, t_{max}, is varied to observe how the result of MEM depends on the t-region used. With decreasing t_{max}, the resolution of the spectral function becomes worse, and for $t_{max} \leq 16$ the spectral function extracted with MEM displays just one peak. Therefore for the circumstances specific at $T > 0$ MEM does not have sufficient resolution to distinguish individual states if they are closer than about $0.05a_\tau^{-1}$. If the correlator is composed of almost free

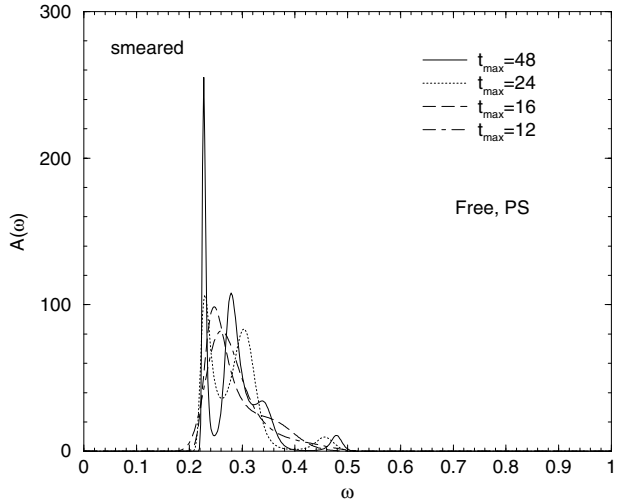

Fig. 2. The result of MEM analysis for the spectral function from the smeared PS correlator composed of free quarks at $T = 0$

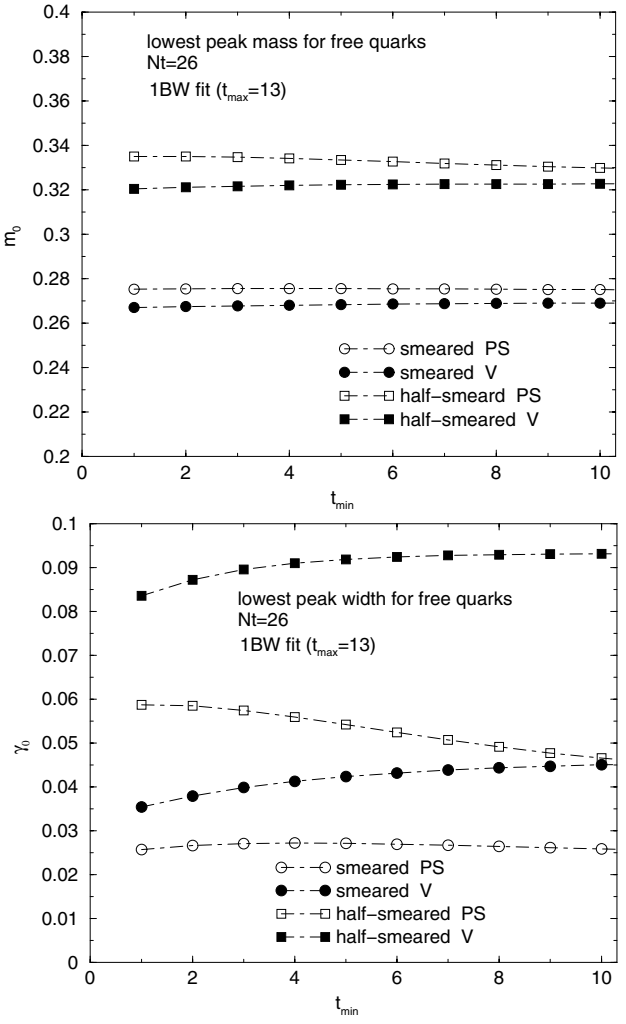

Fig. 3. The result of χ^2 fit analysis for the spectral functions from the PS correlators composed of free quarks at $N_t = 26$

quarks, the width extracted with MEM may be of order of 0.05–0.1 in temporal lattice units.

We also apply the χ^2 fit analysis to the correlators composed of free quarks. In this case the errors of the same size as in Monte Carlo simulation are just put on the correlators without fluctuating them. Figure 3 shows the result of the χ^2 fit of the correlators composed of free quarks at $N_t = 26$ using the 1-BW *ansatz*. The t_{min} dependence of mass and width (with fixed $t_{max} = 13$) indicates that the single BW *ansatz* describes rather well the correlators. As is observed in Fig. 3, if the correlator is composed of free quarks, the χ^2 fit gives sizable difference in mass and width parameters for the smeared and half-smeared correlators. This dependence is in agreement with the fact that the propagator should only show the two free quark cut and no particle-like excitations and indicates that by testing the dependence of the result on the smearing function we can distinguish physical effects from artifacts due to smearing.

5 Setup of numerical simulation

5.1 Lattice setup

The zero temperature lattice used in this paper is the third one of [24]: a quenched lattice of size $20^3 \times 160$, generated with the standard plaquette action with $(\beta, \gamma_G) = (6.10, 3.2108)$. These coupling and bare anisotropy correspond to the renormalized anisotropy $\xi = a_\sigma/a_\tau = 4$ within 1% accuracy [27], and the spatial lattice cutoff $a_\sigma^{-1} = 2.030(13)$ GeV set by the hadronic radius r_0 [28]. At $T = 0$, 500 configurations are generated with the pseudo-heat-bath update algorithm, each separated by 2000 sweeps after 20000 sweeps for thermalization. The mean-field values are defined as the average values of link variables in the Landau gauge, and obtained as $u_\sigma = 0.8059(1)$ and $u_\tau = 0.9901$.

To determine the critical temperature, we measure the Polyakov loop susceptibility at $N_t = 27$, 28, and 29 at $\beta = 6.10$, and in addition, at several values of β (with corresponding values of γ_G) around $\beta = 6.10$ at fixed $N_t = 28$. At $\beta = 6.05$ the lattice scale set by r_0 is $a_\sigma^{-1} = 1.892(10)$ GeV, which together with a_σ^{-1} at $\beta = 6.10$ determine the scales at the other values of β by linear interpolation. The susceptibility peaks at about $\beta = 6.10$ and $N_t = 28$. The critical temperature is obtained as $T_c \simeq 290$ MeV with 10 MeV of roughly estimated uncertainty. This value is slightly higher than the conventional values with the scale set by the string tension, as a common tendency by adopting the scale by r_0.

The charmonium correlators at $T > 0$ are measured for two values of temporal lattice extent, $N_t = 32$ and 26. Corresponding temperatures are $0.88T_c$ for $N_t = 32$, and $1.08T_c$ for $N_t = 26$. For brevity, these temperatures are hereafter referred to as $0.9T_c$ and $1.1T_c$, respectively. Thus the temperatures treated in this paper are in the vicinity of the transition. At each of these two N_t's, we generate 1000 configurations each separated by 500 pseudo-heat-bath sweeps after 20000 sweeps for thermalization.

Table 1. The spectrum at zero temperature determined from the point and the smeared correlators. The masses in PS and V channels are determined with the two-pole fit

Correlator	State	m_{PS}	m_V
Point	ground	0.36835(37)	0.37748(49)
	first exc.	0.449(31)	0.463(42)
	fit range	45–80	50–80
Smeared	ground	0.36856(9)	0.37769(12)
	first exc.	0.500(22)	0.479(23)
	fit range	17–80	15–80

At $N_t = 26$, we find that the configurations almost stay in a single Polyakov loop sector during the whole updating history. Transitions to other sectors occurred only once after more than 470k sweeps. In [7] it was reported that the light mesonic correlators behave differently on configurations in different sectors. We regard quenched lattices as approximations to lattices with dynamical quarks, on which $\mathbf{Z}_3$ center symmetry is explicitly broken and Polyakov loop prefers to stay on the real axis. Therefore we transform all the configurations to the real sector of the Polyakov loop.

5.2 Charmonium correlators

As mentioned in Sect. 3.2, we use $(\kappa, \gamma_F) = (0.112, 4.00)$, which correspond to $m_Q \simeq 0.98$ GeV, roughly the charm quark mass. The statistical errors for the results are estimated with the jackknife method with appropriate binning.

In the next section, we start our analysis at $T = 0$ with the examination of the point correlators. On each configuration, we calculate the point correlators four times with four different source points: $t = 0$ and 80 at spatial site $\mathbf{x} = (0, 0, 0)$ and $t = 40$ and 160 with $\mathbf{x} = (10, 10, 10)$. Then these correlators are averaged with appropriate shifts in t-direction. At $T = 0$ the standard χ^2 fit of data to a multipole form works well. To fix the general picture we anticipate on the analysis of the next sections and list in Table 1 the result of two-pole fits of the point correlators in PS and V channels. The fit ranges $[t_{min}, t_{max}]$ are determined by varying t_{min} with fixed $t_{max} = 80$ and observing the stability of the fit parameters. The results of the ground state masses are very close to the experimentally observed charmonium masses. On the other hand, the hyperfine splitting of about 74 MeV is smaller than the experimental value, $m_{J/\psi} - m_{\eta_c} \simeq 117$ MeV. This is a well-known feature of the quenched lattice simulations and is considered mainly due to quenching, although lattice artifacts in the charmonium system can also play an important role [30].

The smeared correlators are the main target of this paper for reasons we already explained. The smearing parameters were described in Sect. 3.2. The result of a fit to 2-pole form is also shown in Table 1. It is well-known

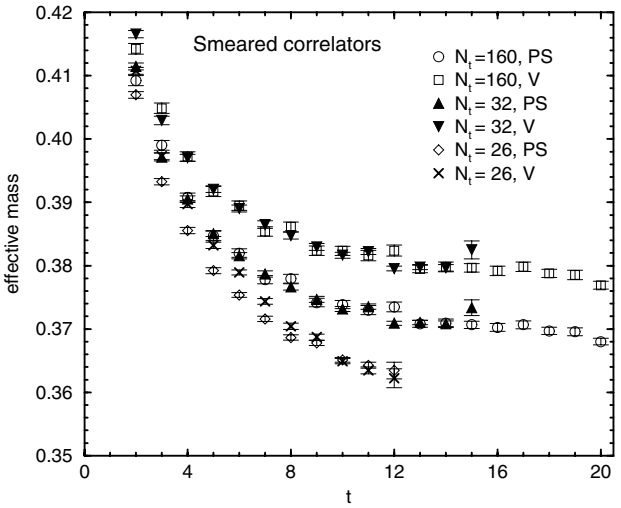

Fig. 4. The effective masses for the smeared correlators in PS and V channels at three temperatures

that the correlators with smeared sink are quite noisy. To reduce the noise, we measure sixteen correlators with different source points on each configuration, and average them. We change the spatial center of the smearing function, as well as the time slice, to reduce the correlation as much as possible. In contrast to a naive expectation, we find this procedure efficient. In fact, at $T = 0$, the statistical errors are reduced by a factor of about 0.3 in the region $t = 8$–16, which is the most important region for the present analyses, in both the PS and V channels. This reduction of errors corresponds to an increase in statistics of about 10 times. Almost the same amount of reduction of errors is observed at $N_t = 32$. At $N_t = 26$, the errors are reduced by factors of 0.40–0.45 in the range $t = 8$–13. This way of reducing statistical errors will be advantageous in the case of dynamical simulations.

For the present kind of analysis, whether the analysis is efficient or not may significantly depends on the statistics. In the temporal region $t = 8$–16, the statistical errors of point correlators at $T = 0$ are about 0.12–0.18% and 0.08–0.15% for PS and V channels, respectively. In the same region, the smeared correlators have statistical errors of 0.14–0.17% and 0.15–0.20%. Therefore at $T = 0$ the errors are of the same order for the point and smeared correlators. At finite temperature, with 1000 configurations, the statistical errors are of roughly the same size as at $T = 0$. We also note that the correlation between the correlators at neighboring time slices is stronger for the point correlators than for the smeared ones.

To obtain an impression of the physics to be expected at various temperatures we show in Fig. 4 the effective mass plot for the smeared correlators, with $m_{eff}(t)$ defined through

$$\frac{C(t)}{C(t+1)} = \frac{\cosh\left[m_{eff}(t)(N_t/2 - t)\right]}{\cosh\left[m_{eff}(t)(N_t/2 - t - 1)\right]}. \qquad (38)$$

If the correlator is dominated by a single (stable) state, $m_{eff}(t)$ shows a plateau. In Fig. 4, the effective masses at

$T = 0$ show plateaus beyond $t \simeq 16$. The effective masses at $N_t = 32$ ($T \simeq 0.9T_c$) show almost the same behaviors as at $T = 0$. This implies that the charmonium states are almost unchanged at this temperature, compared to those at $T = 0$. In contrast, $m_{eff}(t)$'s at $N_t = 26$ ($T \simeq 1.1T_c$) show quite different behavior: they decrease rapidly compared to those at $T < T_c$, and in the large t region ($t \geq 10$) the pseudoscalar and vector channels are almost degenerate. Therefore a qualitatively different behavior of the spectral function is expected below and above T_c. These features are consistent with observations in earlier work [8].

6 Analysis at zero temperature

6.1 Result of MEM for point correlators

We start with MEM analysis of the point correlators at zero temperature.

First we discuss the default model function. Following previous applications of MEM to lattice data [9,13], we adopt as m_{DM} in (32) the asymptotic values of correlators in the perturbative QCD,

$$\frac{1}{\omega^2} A^{cont}(\omega \gg \Lambda_{QCD}) = \frac{r_1}{4\pi}\left(1 + r_2 \frac{\alpha_s}{\pi}\right), \qquad (39)$$

where $r_1 = 3/2$ and $r_2 = 11/3$ for PS channel, and $r_1 = 1$ and $r_2 = 1$ for V channel. As value of the strong coupling constant α_s, we use $\alpha_s = 0.2$ at 8 GeV from [31] as a typical value at the temporal cutoff of the present lattice. The matching of the lattice theory with the continuum theory is performed through the tadpole-improved tree-level, and hence the renormalization of the quark field is represented only by the KLM normalization factor (22). These settings give for the parameter of the default model function $m_{DM} = 4.1$ for PS channel, and 2.4 for V channel. If MEM works as a method to extract the spectral function without assuming a specific form, the result should not be sensitive to the choice of this parameter. In addition, the observed asymptotic behavior of the spectral function from lattice data around the cutoff is actually different from that of (39) [32]. We therefore observe the dependence of the result on the value of m_{DM} by changing m_{DM} by factors of 10 and 0.1, to verify the insensitivity of the result to m_{DM}.

The further setting of MEM is as follows. In all cases, the correlator at $t = 0$ is not used for the analysis. The minimum of t used depends on the type of analysis, in most cases $t_{min} = 1$ is adopted. The frequency ω is discretized with $\Delta\omega = 0.002$, in the region $[\omega_{min}, \omega_{max}] = [0.001, 4.0]$. The dependence of the result on the parameters for ω is sufficiently small around the adopted values.

We first examine how the restriction of degrees of freedom of the correlator affects the reconstructed spectral function. Three parameters t_{min}, t_{max} and t_{sep} are introduced, that is MEM is applied for the correlators at times $t_{min} \leq t \leq t_{max}$ in every t_{sep} time slices. We examine two types of restrictions of the numbers of degrees of freedom:

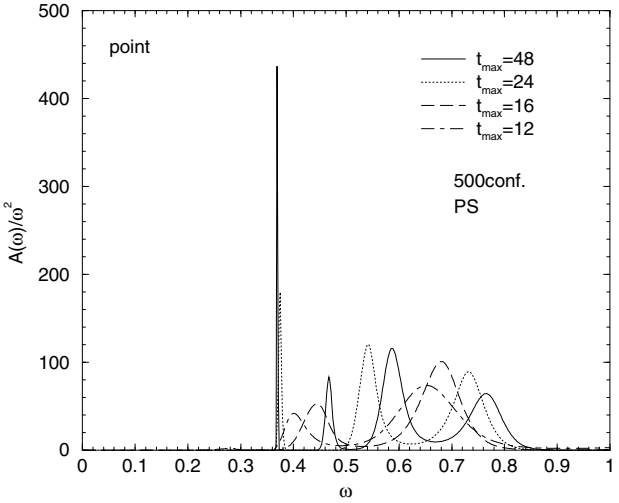

Fig. 5. The result of MEM analysis of the point correlator in PS channel at $T = 0$. The figure shows the t_{max} dependence of the resultant spectral function

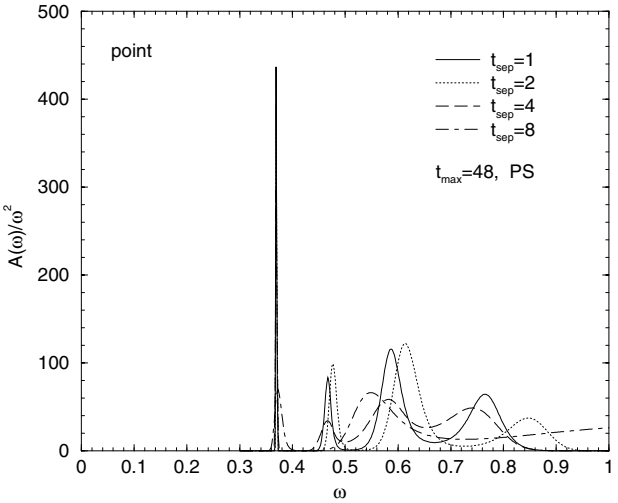

Fig. 6. The result of MEM analysis of the point correlator in PS channel at $T = 0$. This figure shows the t_{sep} dependence of the result of the spectral function with fixed $t_{max} = 48$

(I). t_{max} is varied as 48, 24, 16, and 12, with fixed $t_{min} = 1$ and $t_{sep} = 1$. The corresponding numbers of data points are the same as t_{max}.

(II). t_{sep} is varied as 1, 2, 4, and 8, with fixed $t_{max} = 48$. t_{min} is varied accordingly as $t_{min} = t_{sep}$. Correspondingly, the numbers of data points are 48, 24, 12, and 6, respectively.

From the point of view of the basis functions of the singular value decomposition in the spectral function space, case (I) reduces the number of basis functions while keeping the functions unchanged. On the other hand, case (II) dilate the basis functions by a factor of t_{sep} simultaneously reducing their number. Reliability of the result at finite temperature requires the obtained spectral function to be stable under the type (I) restriction. Although larger values for t_{max} are possible, $t_{max} = 48$ is sufficiently large

and has appropriate physical range ($t_{max}a_\tau \simeq 1.2$ fm) for the present purpose.

The result is shown in Figs. 5 and 6 for the pseudoscalar channel. For the vector correlator a similar result is obtained. In the case of $t_{max} = 48$ and $t_{sep} = 1$, i.e. without restriction, the reconstruction of the spectral functions seems successful, and their fundamental features appear to be the same as in previous works [9,13]. The peak positions of the ground and first excited states are consistent with the result of χ^2 fit summarized in Table 1. Here we do not discuss the higher excited states because of uncertainties not only in MEM but also in the χ^2 fit analysis.

Figure 5 displays the result under restriction conditions (I). Decreasing t_{max}, the spectral function becomes increasingly different from that with $t_{max} = 48$. For $t_{max} \leq 24$, the first excited state peak does not appear at the correct place, and for $t_{max} \leq 16$ even the ground state peak is located at an incorrect place and has broad width. These lowest peaks for different t_{max}'s are all significant in the sense of the error analysis of MEM [9]. Therefore $t_{max} \leq 16$ is not acceptable for extracting reliable information of the ground state from the point correlators. Since at finite temperature we are restricted to $t_{max} \leq 16$ because of short temporal extent this is the reason why we abandon using the point correlators and apply the smearing technique.

Figure 6 shows the result with restriction condition (II). In this case, the reconstructed spectral functions are rather stable, while the sharpness of peaks is lost by increasing t_{sep}. Even with 6 degrees of freedom (as a linear combination of 6 functions), the reconstructed spectral function at least exhibits the ground state peak at the correct position. To summarize, if one has a temporal region of the correlator of the order of 1 fm, the spectral function can be rather nicely reconstructed even with less than 10 degrees of freedom.

From these observation, we conclude that with $O(10)$ degrees of freedom the crucial condition is determined by the region of t where the correlators are measured. $t_{max}a_\tau$ of the order of 1 fm seems necessary for a reliable extraction of the spectral function from the point correlator. Increasing the number of degrees of freedom above 10 with fixed physical range of $[t_{mim}, t_{max}]$ improves the situation only slightly.

Now we consider the effect of the statistics. We apply the same analysis of the case (I) restriction to the correlators averaged over first 100 configurations. The observed features of t_{max} dependence are essentially the same as with 500 configurations. Therefore at the present level of statistics (order of several hundreds), increasing statistics does not seem to improve drastically the situation of the t_{max} dependence. We also compare the correlators averaged over 100 configurations randomly selected from the total of 500 configurations. A comparison of the results with $t_{max} = 48$ from five such correlators shows that the first excited state does not always appear at the same place as with 500 configurations, but deviates in a range of $\omega = 0.44$–0.52. Thus with less statistics only the ground state peak can be trusted even with $t_{max} = 48$. These observations indicate the required statistics for each situation.

Finally we briefly discuss the dependence on the default model. We compare the results obtained with m_{DM} in (32) multiplied by 10 and 0.1 with otherwise fixed parameters, $t_{max} = 48$ and $t_{sep} = 1$. These results of the spectral function display the peaks at the same places as with original m_{DM}, while increasing m_{DM} the peaks become sharper. Although present analysis is quite simple, we conclude that the default model dependence of the result of MEM is not severe, at least for a rough estimate of the shape of the spectral function.

The most important conclusion in the analysis of the point correlator is that we need the order of 1 fm for the range of t where the correlators are measured, for reliable extraction of the spectral function from the correlator with present level of statistics. This requirement cannot be fulfilled at finite temperature, and a brute force application of MEM to the point correlators at $T > 0$ would produce an unreliable result. This result warns us against physical significance of the results in [16,17,18,19]. This difficulty may originate in that the point correlator at short distance contains the contribution from wide range of frequency up to the lattice cutoff. We therefore give up to analyze further the point correlators, and concentrate our attention on the smeared correlators.

6.2 Result of MEM for smeared correlators

We now turn to MEM analysis of the smeared correlators. Since the smearing technique reduces the high frequency part, there is no a priori choice for the form of the default model. As described in Sect. 4.2, we use the same default model function as for the point correlator, with the normalization of the smeared correlator which gives the same overlap with the ground state as the point correlator. The default model dependence is examined in the same manner as for the point correlators. Other parameters are the same as for the point correlator, except that $\omega_{max} = 2.0$ is adopted, since the high frequency region is sufficiently suppressed.

First we examine the dependence of the result on the numbers of degrees of freedom, using the same restriction conditions as for the point correlators. Since the smearing technique enhances the low energy part, we only consider whether the ground state peak is correctly reproduced or not. The result for the restriction condition (I) is displayed in Fig. 7. In the both cases of PS and V channels the place of the ground state peak is stable with decreasing t_{max}, although the width is gradually broadened. Since the ground state peak evidently has no physical width at $T = 0$, this fictitious width is a systematic uncertainty of MEM due to the insufficient number of basis functions in the spectral function space. Therefore, in particular at finite temperature, an estimate of the physical width requires a careful analysis combined with other procedures. The instability of the first excited state peak under changing t_{max} is explained by the smallness of the contribution

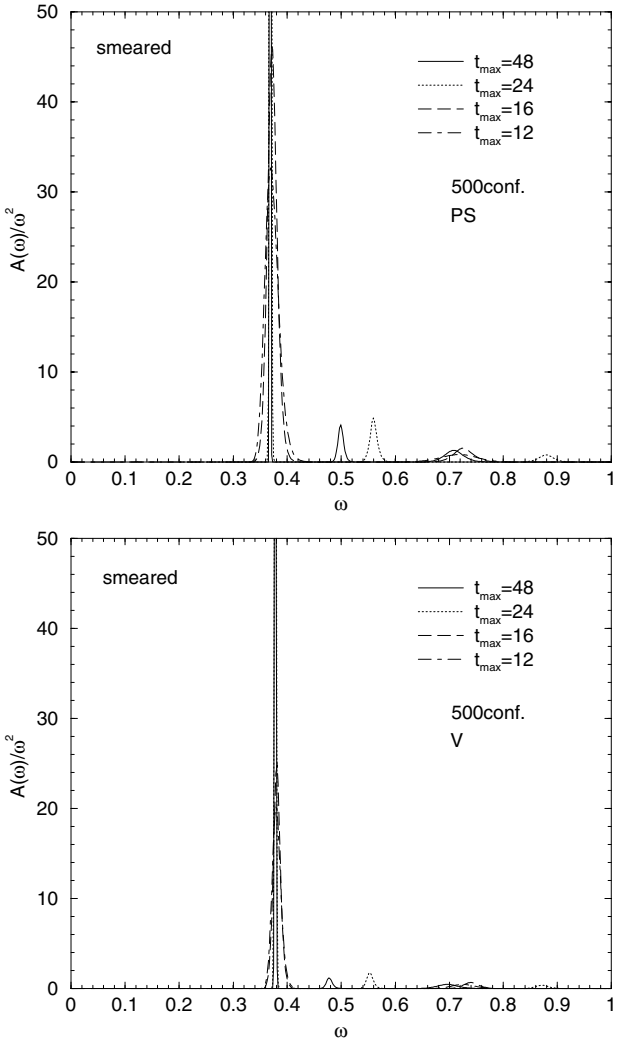

Fig. 7. The spectral functions at $N_t = 160$ determined with MEM. The *top and bottom panels* show the t_{max} dependences of obtained spectral functions in PS and V channels, respectively

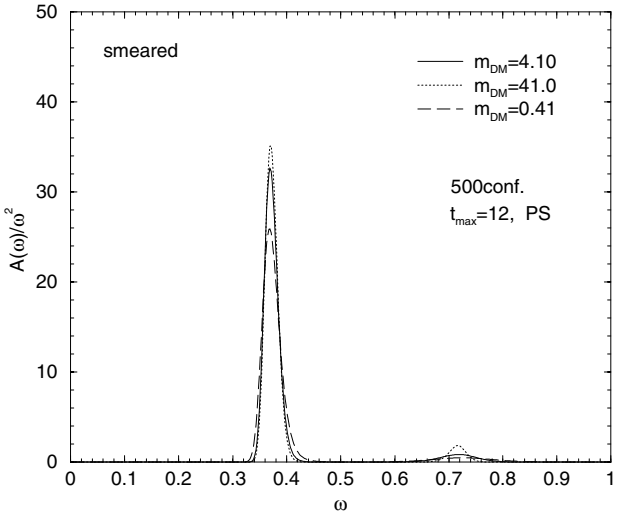

Fig. 8. The default model dependence of the extracted spectral function with MEM from the smeared correlators in PS channel. The figure shows the result of MEM with three values of m_{DM}, the parameter of the default model function (32)

to the correlators from energies above the ground state. In fact, the two-pole fit analysis indicates that the overlap of the first excited state with the smeared correlator is about 7% (6%) of that of the ground state for the PS (V) channel. Thus the instability of the excited state peaks has no significance for the following analysis. We conclude that for the smeared correlators, MEM with $t_{max} \simeq 12$ would work for a rough estimate of the structure of the spectral function in the low energy part, such as examination of whether strong ground state peak exist, while a quantitative evaluation of width, for example, is difficult. In the case of the restriction condition (II), a similar tendency as for the point correlators is observed: the position of the ground state peak is stable with increasing t_{sep}, while the sharpness of the peak is gradually lost.

The m_{DM} dependence of the result is examined in two cases of t_{max}, $t_{max} = 48$ and 12, by using rescaling factors 10 and 0.1. In the case of $t_{max} = 48$, the ground state peak is strong, and changing m_{DM} does not cause a large effect other than the decrease of the peak height with slight increase of the width when decreasing m_{DM}. Figure 8 shows the case of $t_{max} = 12$ for the PS channel. Although the peak shape is broadened with decreasing m_{DM}, the essential features of the result are stable. A similar result is observed for the V channel.

Let us summarize the MEM analysis of the smeared correlators at $T = 0$. In contrast to the case of the point correlators, MEM with restricted numbers of degrees of freedom works up to $t_{max} = 12$, i.e. $t_{max} a_\tau \simeq 0.3$ fm, at least for a rough estimate of the shape of the spectral function in the low energy part. For this purpose, systematic uncertainties in the default model parameter do not appear significant. This is an encouraging result for an application of MEM to finite temperature as a precedent analysis to the χ^2 fit.

6.3 Result of χ^2 fit analysis

The results with 2-pole *ansatz* have been given in Table 1. For completeness, we also apply the χ^2 fits to the smeared correlators with forms other than the 2-pole fit. The result is shown in Fig. 9. As fit range $[t_{min}, t_{max}]$ we fix $t_{max} = 13$, considering the severest case at $T > 0$, and observe the t_{min} dependence of the result. The top and bottom panels of Fig. 9 show the results of mass and width of the ground state peak, respectively. The fit result for the ground state mass is slightly larger than that of the full data analysis with $t_{max} = 80$ in Table 1. This deviation indicates a typical size of the systematic uncertainty caused by the short fit ranges.

As is expected, the 2-pole form describes well the correlators, and the other two fit forms are consistent with the 2-pole fit. In the cases of 1-BW and BW+pole fits

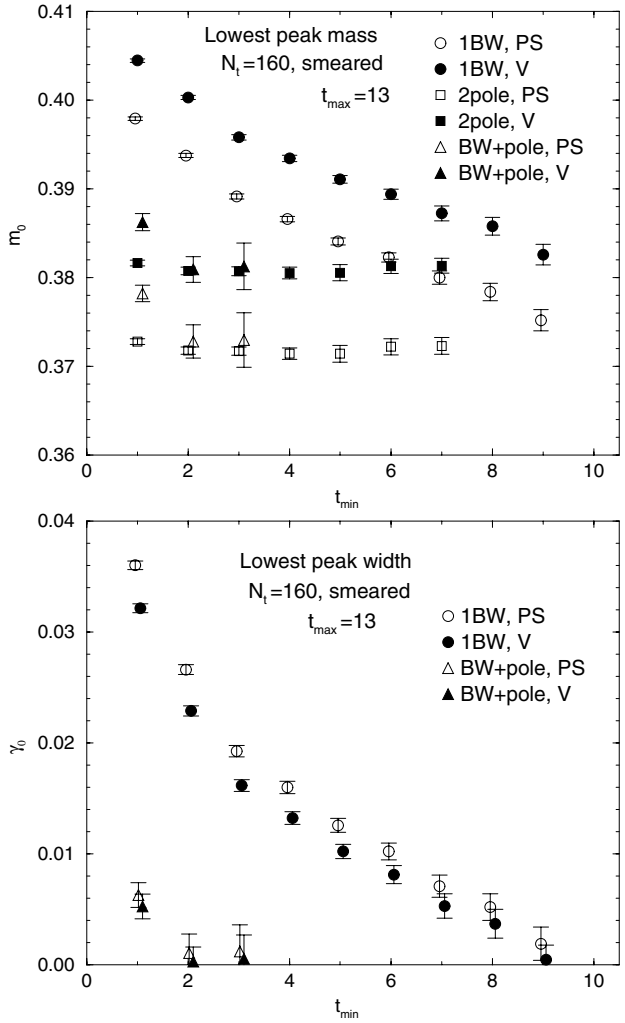

Fig. 9. The result of the χ^2 fit analysis at $N_t = 160$. The top and bottom panels show the results for mass and width of the ground state peak, respectively

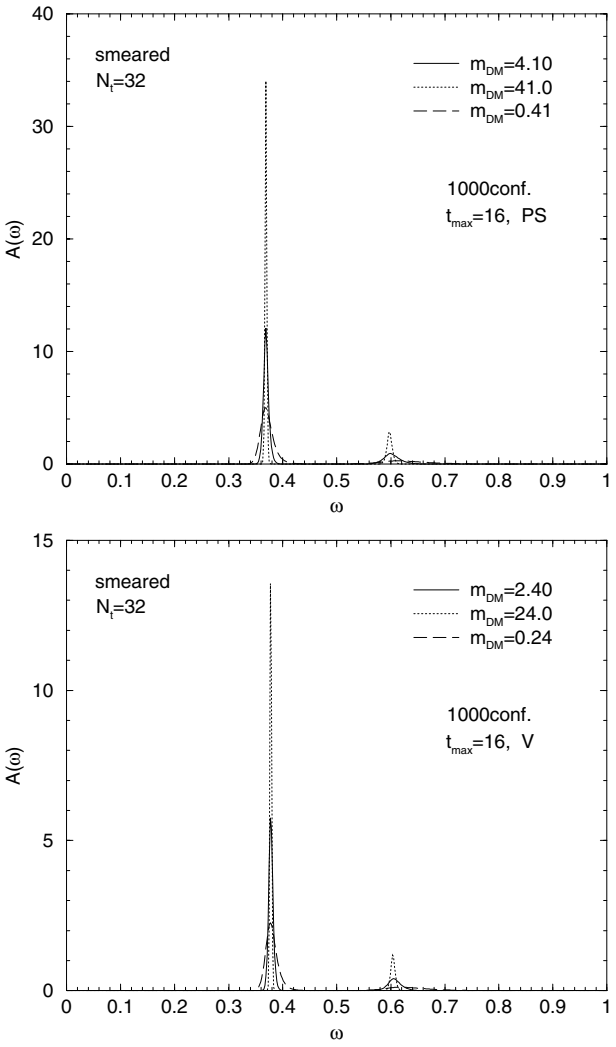

Fig. 10. Spectral functions at $N_t = 32$ determined with MEM

the t_{min} dependences of the widths are significant. In the bottom panel the results for the width decreases as t_{min} increases, and seem to approach zero. Therefore no indication of a finite width is found at $T = 0$, as it should be.

7 Analysis at $T < T_c$

Now the two analysis procedures are applied to the correlators at $T \simeq 0.9T_c$ ($N_t = 32$). In this and the next sections we no longer discuss the point correlators and focus only on the smeared ones.

7.1 Result of MEM analysis

We begin with the MEM analysis, in accordance with our strategy. The parameters concerning MEM are almost the same as for the smeared correlators at $T = 0$. The range of t is fixed to $t_{min} = 1$, $t_{sep} = 1$, and $t_{max} = 16$.

The result is displayed in Fig. 10 for three values of m_{DM}. For the reasons already mentioned we focus on the ground state peak and do not discuss in detail the high frequency part of the spectral function. As apparent in the figure a ground state peak appears in both the PS and V channels. Although with decreasing m_{DM} the widths of the ground state peaks increase, the positions of the peaks are stable and almost the same as at $T = 0$. In the present case, since there is no intrinsically advisable value for m_{DM} beyond an order estimate, this ambiguity of the width of the peak should be considered as an uncertainty of MEM applied to the smeared correlators. We also perform the same analysis with less statistics, 500 configurations, to see how this result depends on the statistics. The result is essentially the same, and thus statistically stable.

These results support the assumption that the mesonic ground states are persistent up to this temperature, with almost the same masses as at $T = 0$. The width of the ground state peaks is small while finite, although it strongly depends on the value of m_{DM}. Whether the width

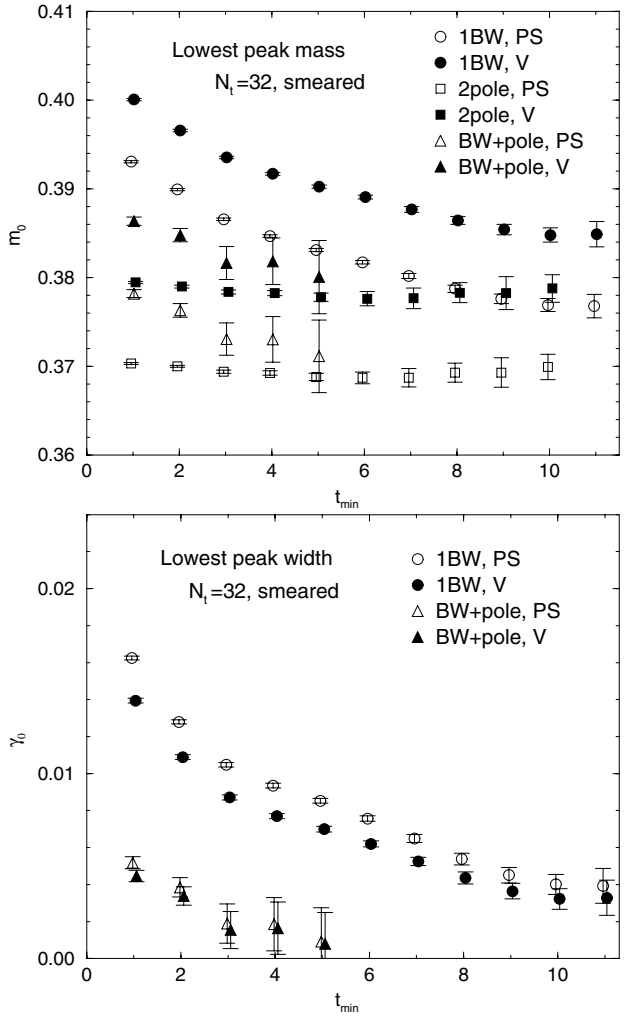

Fig. 11. The result of χ^2 fit analysis at $N_t = 32$. The *top and bottom panels* show the results of the mass and width parameters for the ground state peak, respectively

is physically finite or not should therefore be examined with the χ^2 fit analysis.

7.2 Result of χ^2 fit analysis

According to the result of MEM we can assume that the spectral function of the smeared correlator at this temperature has a peak structure at almost the same mass as at $T = 0$ and with small width. Therefore it is expected that the χ^2 fits with the three types of fit forms, 2-pole, 1-BW, and BW+pole forms can clarify the low energy structure of the spectral function.

The results are summarized in Fig. 11. The top panel displays the dependence of the mass parameters for the ground state peak on the lower bound of the fit range, t_{min}. The upper bound is fixed to $t_{max} = 16$. It is apparent that the fit to the 2-pole form exhibits stable results both for the PS and V channels beyond $t_{min} = 3$. The result of fit to 1-BW form exhibits no plateau, indicating that this form does not explain the whole structure of the correlators. However, the values seem to approach to the corresponding results of the 2-pole fits. The result of fit to the BW+pole form is consistent with those of 2-pole fit at $t_{min} \leq 2$.

The bottom panel of Fig. 11 shows the result for the width parameter. In the case of the fit to the 1-BW form the value of width gradually decreases with increasing t_{min}. This behavior is consistent with a vanishing width. The fit to BW+pole form also indicate that the width is consistent with zero. Therefore, there is no indication of a finite width for the spectral function at this temperature.

All the results of fits to the three forms indicate that the ground state peak is well described by a strong peak with vanishing width, i.e. a pole-like structure, and the associated mass is almost the same as at zero temperature.

8 Analysis at $T > T_c$

8.1 Result of MEM analysis

In this section, we analyze the correlators at $T \simeq 1.1T_c$ ($N_t = 26$).

The setup of MEM analysis is the same as at $T \simeq 0.9T_c$, except for $t_{max} = 13$. Figure 12 shows the result. In both the PS and V channels there appear strong peak structures around $\omega \simeq 0.4$. This peak, hereafter called "the ground state peak" for simplicity, appears at almost the same position as at $T \simeq 0.9$ but with larger width. Although, as a common tendency, the peak becomes sharper as the default model parameter m_{DM} increases, the position of the peak is unchanged. It is also verified that the result is essentially the same with less statistics, namely 500 configurations. Therefore it is presumable that the spectral function still has a peak structure at almost the same position as below T_c.

This result should be compared with the case where the correlators are composed of free quarks, considered in Sect. 3.3. In the latter case, as shown in Sect. 4.4, MEM with the present number of degrees of freedom may produce the same feature of the spectral function but with a lower peak position. The above result therefore does not exclude the possibility that the correlators are composed of two weakly interacting quarks with rather large effective mass.

To judge between almost free quarks and genuine bound-state-like structure we analyze the half-smeared correlator. We repeat the same analysis as applied to the smeared correlators for the half-smeared correlators and verify that MEM works up to $t_{max} = 12$ on almost the same level as for the smeared ones. As discussed in Sect. 4.4, if the correlator is composed of two almost free quarks the extracted spectral function should exhibit now a wider peak at a higher position. Figure 13 shows the result of MEM analysis for the half-smeared correlators. The analysis is performed in the same manner as for the smeared correlators. Comparing with the result for the smeared correlator, the peak position for the half-smeared one is almost unshifted, while the width of the peak tends to broaden slightly. The latter effect , however, can also be

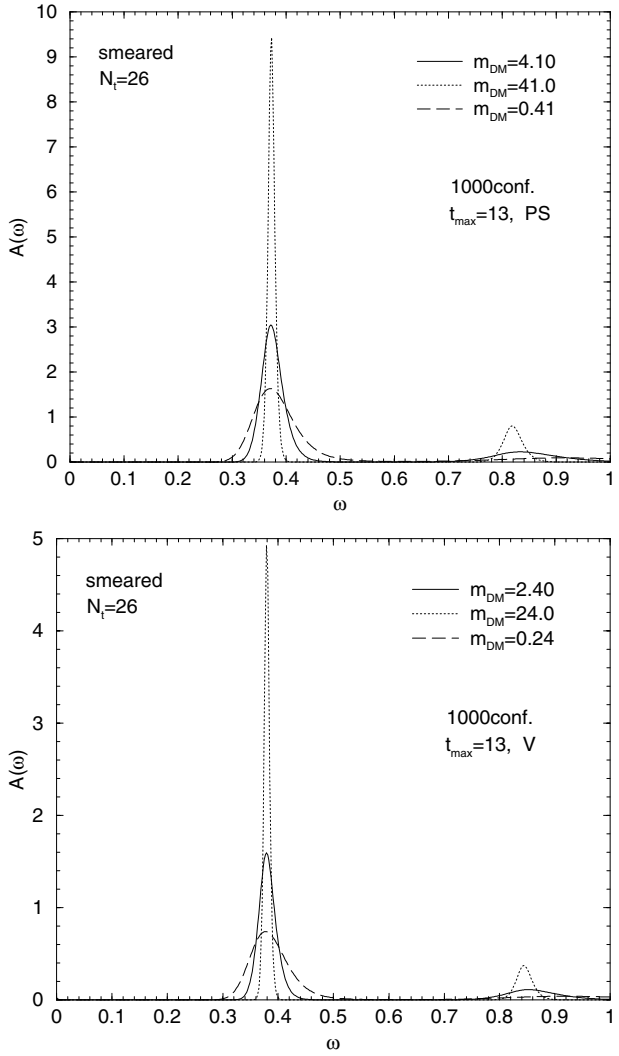

Fig. 12. The spectral function at $N_t = 26$ determined with MEM (smeared correlators)

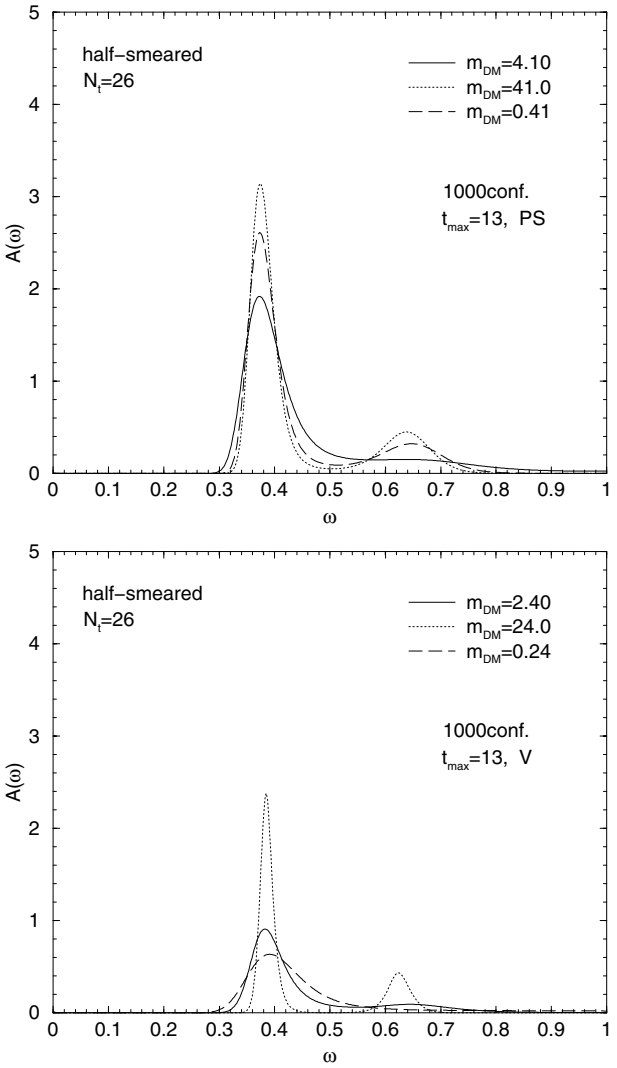

Fig. 13. The results of MEM for the spectral function of the half-smeared correlators at $N_t = 26$

explained as an effect of default model uncertainty. This result is therefore not in accord with the assumption that the peak structure is an artifact of the smearing. Hence the MEM analysis supports a bound-state-like structure at this temperature.

8.2 Result of χ^2 fit analysis

According to the result of MEM, it is reasonable to assume that the spectral function of the smeared correlator at this temperature also have a peak structure, similarly to the $T < T_c$ case. Therefore the three forms for the χ^2 fit analysis are still reasonable assumptions to investigate the low energy structures of the correlators.

Figure 14 shows the result of the χ^2 fit analysis for the smeared correlators. The top panel shows the t_{min} dependence of the mass parameters. In contrast to the case below T_c, the masses from 2-pole fit no longer approach those of the other two fit forms but fall monotonously. The masses from 1-BW and BW+pole fits exhibit consistent behaviors, indicating that these fits represent better the correlators. Actually the values of χ^2/N_{DF} are consistently fluctuating around unity at $t_{min} > 8$ for 1-BW fit, and in the whole range of t_{min} for BW+pole fit. In the BW+pole fit, the mass parameters for the second peaks take values around 0.9 and 1.0 for PS and V channels, respectively, which is roughly consistent with the result of MEM. The consistency of 1-BW and BW+pole fits also holds for the width parameters, as displayed in the bottom panel of Fig. 14. These results indicate therefore that the widths associated with the ground state peaks are finite for both the correlators in PS and V channels.

We now analyze the half-smeared correlators to examine whether this observation of peak structure is an artifact of the smearing. The analysis is performed in the same manner as for the (fully) smeared correlators. The result is displayed in Fig. 15. The mass parameters for the half-smeared correlators (top panel) show a similar ten-

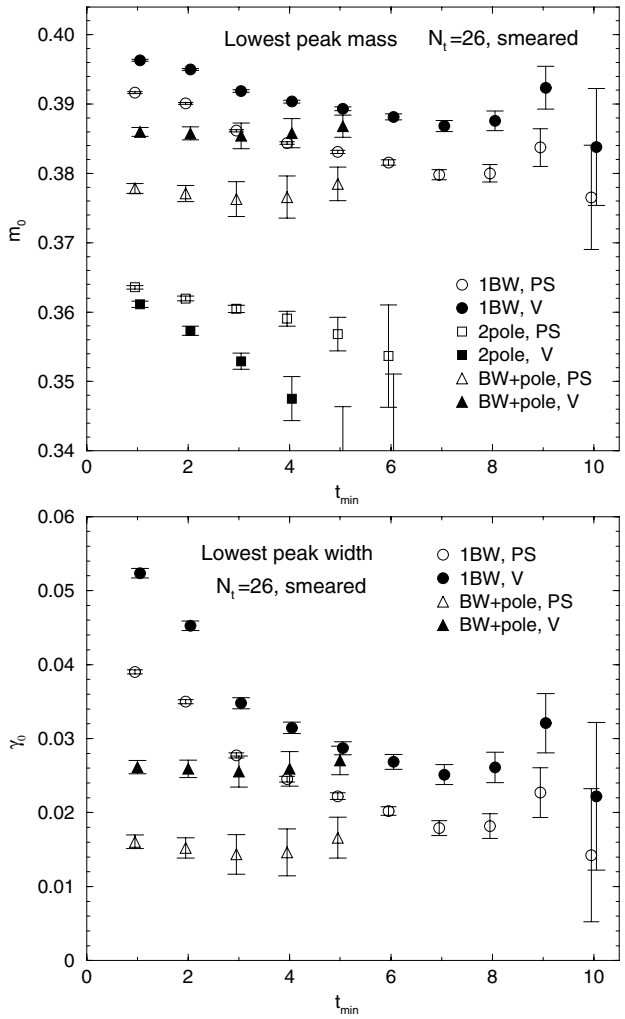

Fig. 14. The result of χ^2 fit analysis for the smeared correlators at $N_t = 26$

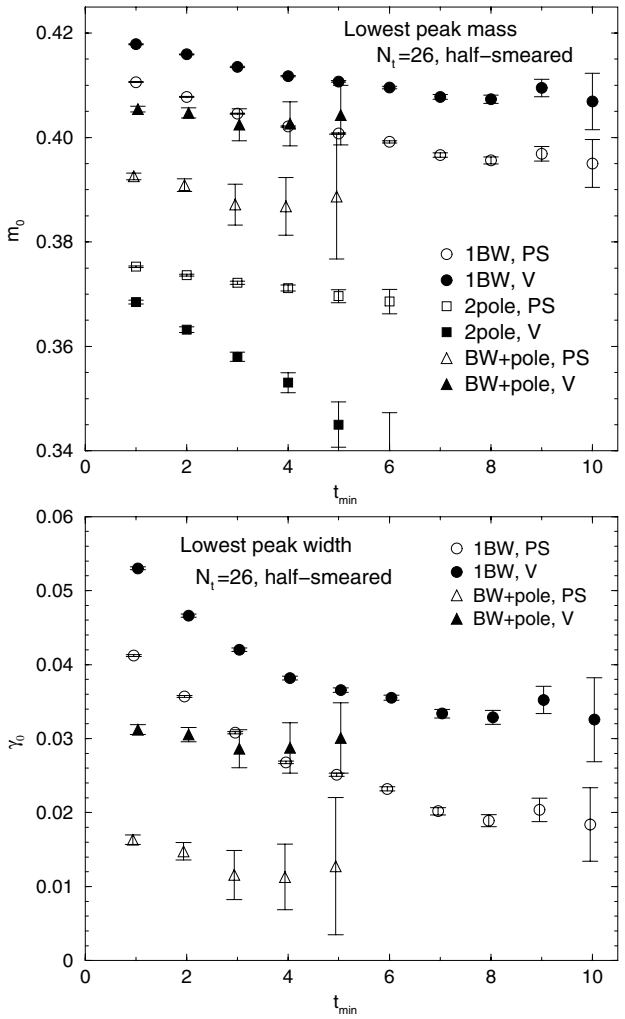

Fig. 15. The result of χ^2 fit analysis for the half-smeared correlators at $N_t = 26$

dency as for the smeared correlators, although the result of 1-BW and BW+pole fits approach slightly larger values than those of smeared correlators. The shifts of the masses are at most 5% and can be explained with the frequency dependence of the overlap $R(\omega)$ in (13). A similar tendency is also found for the width parameters in the bottom panel of Fig. 15, which appear even more consistent with those of smeared correlators than the mass parameters.

Figure 16 illustratively compares these spectral functions extracted with the χ^2 fits from four kinds of correlators: the smeared and half-smeared correlators, numerically measured and composed of free quarks. The results of the numerical simulation are of the BW+pole fit with $t_{min} = 4$. For the free quark case the results of 1-BW fit with $t_{min} = 8$ is displayed. We note that the normalizations of the spectral functions are not significant in the present analysis. In both the PS and V channels the spectral functions for the numerically observed correlators strongly peak near $\omega = 0.4$ with small widths. If a peak structure is of genuine physical, the shift of peak position caused by a change of smearing function must be within the width of the peak. This is in fact the case in the result of numerical simulation. However in the free quark case, in PS channel, the peak position from the fit changes beyond the width of smeared operator as shown in Fig. 16 (see also Fig. 3). For the vector channel, in which the fit analysis of correlators composed of free quarks gives larger widths than PS channel, the shift of peak caused by the change of smearing function is also much less than the case of free quarks. As noted at the end of Sect. 3.3, the quantum effect may smoothen the spectral function in the case of almost free quarks. Even taking this effect into account, the sizable shift of mass and the broadening of width observed in the free quark case are not observed in the result of numerical simulation. It is difficult to exclude completely the possibility that the correlators are composed of almost free quarks with rather large effective mass and nontrivial dispersion relation. However, it is quite suggestive that a nontrivial structure indicating the existence of bound-state-like structure in the low energy region of spectral function subsists at this value of T.

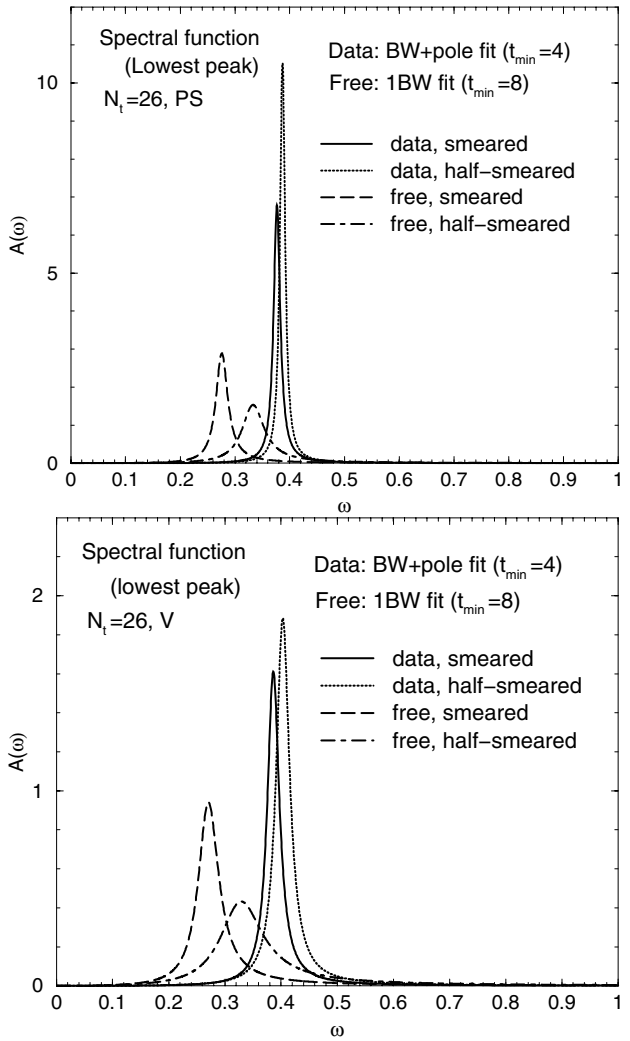

Fig. 16. The spectral functions obtained with χ^2 fit analysis at $N_t = 26$. For the correlators composed of free quarks only the result of BW fit is displayed, while a BW+pole fit is used for the correlators measured in the simulation

Summarizing the results of MEM and χ^2 fit analysis we conclude that the charmonium correlators in PS and V channels at $T \simeq 1.1T_c$ possess a nontrivial peak structure in the low energy region. As representative values of m_0 and γ_0, we quote the results of the BW+pole fit analysis with $t_{min} = 4$ for the smeared correlators:

$$\text{PS}: \ m_0 = 3.06(2) \text{ GeV}, \quad \gamma_0 = 0.12(3) \text{ GeV}, \quad (40)$$

$$\text{V}: \ m_0 = 3.13(2) \text{ GeV}, \quad \gamma_0 = 0.21(2) \text{ GeV}. \quad (41)$$

The quoted errors in m_0 and γ_0 are only the statistical ones. As obvious from the discussions in this sections, these results should contain systematic uncertainties of the order of 5% due to the analysis procedures, apart from other uncertainties such as finite lattice artifacts and quenching effects. Compared with the result at $T \simeq 0.9T_c$, the widths at $T \simeq 1.1T_c$ is sizable, indicating a genuine temperature effect in the deconfined phase. On the other hand, the masses are almost unchanged.

9 Conclusion

The main goals of this paper were (1) to elucidate the technical problems in extraction of the spectral function from lattice data of t-correlators, and (2) to investigate the temperature effect on the spectral function near the deconfining phase transition. In the following, we summarize and discuss the results obtained in this paper.

As techniques to extract the information on the spectral function we examined maximum entropy method (MEM) and the standard χ^2 fit assuming suitable forms of the spectral function. It is essential to check the reliability of the applied methods to the systems in question. Our condition for reliability at finite temperature is that the methods reproduce the correct form of the spectral function at $T = 0$ when the t-interval is restricted to the one forced on us at $T > 0$. We examined MEM by applying it to the point and smeared correlators. We find that MEM does not meet this requirement for the former, while it does for the latter. This is understandable, since the smearing enhances the low energy part of the spectral function, which is what we are interested in, while a much wide energy region contributes to the point correlators. We note that whether MEM correctly works or not depends primarily on the extension of the physical t-region. In particular, for the point correlators a region of t of $O(1\text{fm})$ is necessary. For the smeared correlator, this condition is much relaxed. Therefore only the smeared correlators were analyzed at finite temperatures.

Since MEM is ambiguous concerning the quantitative detail of the spectral function, the latter should be also analyzed with other procedures. As such a procedure, the χ^2 fit is a reasonable candidate, since MEM already gives a hint for a suitable *ansatz* for the spectral function. With several assumed forms and examining the fit range dependence of the resultant values for the parameters, this procedure gives us more quantitative information on the properties of spectral function. We emphasize that MEM and χ^2 fit analysis as used here are complementary to each other. This two-step approach actually worked for analyses of the correlators at finite temperature, as well as at $T = 0$.

Now we discuss the physical implications of our results below and above the critical temperature. We remind that our numerical simulation was performed without dynamical quark effects.

Below the deconfining temperature, at $T \simeq 0.9T_c$, the reconstructed spectral function has a strong peak corresponding to the ground state, with almost the same mass as at $T = 0$ and narrow width consistent with zero. In contrast to the potential model analysis [1], the charmonium mass is not changed up to this temperature. Similar tendencies have been reported in previous lattice QCD calculations for the mesonic channels [7,8], while sizable reduction of mass has been observed for glueballs [20]. Considering the rather quantitative success of the potential model approach for the charmonium systems at $T = 0$ [34], it is important to explain this discrepancy.

At $T \simeq 1.1T_c$ we observed an indication that the spectral functions still has strong peaks at almost the same

positions as $T < T_c$, and with widths of about 0.12 and 0.21 GeV for PS and V channels, respectively. This result presumably indicates the existence of quasi-stable bound-state-like structures persistent up to this temperature. The possibility of observing correlators composed of almost free quarks (but of large effective masses) is, however, not completely excluded. The observations are not in accord with the expectation from the naive potential model approach [2,33]. Up to around $1.1T_c$, however, it has been pointed out that bound states may exist in a potential model analysis based on recent lattice QCD data of static potential [35]. In either case, our result implies that the plasma phase has a nontrivial structure at least near the critical temperature.

For a more definite understanding of hadronic correlators at $T > 0$ more studies containing dynamical simulations are necessary, as well as calculations in wider range of temperatures. The techniques adopted in this paper should in principle be applicable to these situations. However, it would become more difficult to distinguish a physical peak structure from an artificial peak brought by the smearing as temperature increases, since the contribution to the correlators from the high frequency part of the spectral function increases and the peak structure may broaden. It is also important to repeat the same sort of analysis in the light hadron sectors, for which a nontrivial structure of correlators above T_c was also reported [7].

Acknowledgements. We would like to express our sincere gratitude to Professor Osamu Miyamura, who tragically passed away in July 2001, for his inspiring us with this work and for valuable discussions. We thank N. Ishii, K. Kanaya, T. Kunihiro, A. Nakamura, T. Onogi, I.-O. Stamatescu, and T. Yamazaki for useful discussions. We are also grateful to the members of QCD-TARO Collaboration; this work was done partly in accordance with their long standing physical goals. The simulation has been done on NEC SX-5 at Research Center for Nuclear Physics, Osaka University and Hitachi SR8000 at KEK (High Energy Accelerator Research Organization). T.U. is supported by the center-of-excellence (COE) program at CCP, University of Tsukuba. H. M. is supported by Japan Society for the Promotion of Science for Young Scientists.

References

1. T. Hashimoto, O. Miyamura, K. Hirose, T. Kanki: Phys. Rev. Lett. **57**, 2123 (1986)
2. T. Matsui, H. Satz: Phys. Lett. B **178**, 416 (1986)
3. NA50 Collaboration, M. C. Abreu et al.: Phys. Lett. B **477**, 28 (2000)
4. For a review, H. Satz: Nucl. Phys. B (Proc. Suppl.) **94**, 204 (2001)
5. A.A. Abrikosov, L.P.Gor'kov, Dzyaloshinskii: Sov. Phys. JETP **36(9)**, 636 (1959); E.S. Fradkin: Sov. Phys. JETP **36(9)**, 912 (1959)
6. T. Hashimoto, A. Nakamura, I. O. Stamatescu: Nucl. Phys. B **400**, 267 (1993); Nucl. Phys. B **406**, 325 (1993)
7. QCD-TARO Collaboration, Ph. de Forcrand et al.: Phys. Rev. D **63**, 054501 (2001)
8. T. Umeda, R. Katayama, O. Miyamura, H. Matsufuru: Int. J. Mod. Phys. A **16**, 2215 (2001)
9. Y. Nakahara, M. Asakawa, T. Hatsuda: Phys. Rev. D **60**, 091503 (1999); M. Asakawa, T. Hatsuda; Y. Nakahara: Prog. Part. Nucl. Phys. **46**, 459 (2001)
10. For pioneering works, QCD-TARO Collaboration, Ph. de Forcrand et al.: Nucl. Phys. B (Proc. Suppl.) **63**, 460 (1998); E.G. Klepfish, C.E. Creffield, E.R. Pike: ibid. 655 (1998)
11. I. Wetzorke, F. Karsch: hep-lat/0008008.
12. M. Oevers, C. Davies, J. Shigemitsu: Nucl. Phys. B (Proc. Suppl.) **94**, 423 (2001)
13. CP-PACS Collaboration, T. Yamazaki et al.: Phys. Rev. D **65**, 014501 (2002)
14. H.R. Fiebig: Phys. Rev. D **65**, 094512 (2002); H.R. Fiebig, LHP collaboration: Nucl. Phys. B (Proc. Suppl.) **106**, 344 (2002)
15. Difficulty in extracting transport coefficients from lattice data has been pointed out in: G. Aarts, J.M. Martinez Resco: JHEP **0204**, 053 (2002); hep-lat/0209033
16. F. Karsch, E. Laermann, P. Petreczky, S. Stickan, I. Wetzorke: Phys. Lett. B **530**, 147 (2002); I. Wetzorke et al.: Nucl. Phys. B (Proc. Suppl.) **106**, 510 (2002)
17. P. Petreczky, F. Karsch, E. Laermann, S. Stickan, I. Wetzorke: Nucl. Phys. B (Proc. Suppl.) **106**, 513 (2002)
18. S. Datta, F. Karsch, P. Petreczky,I. Wetzorke: hep-lat/0208012
19. M. Asakawa, T. Hatsuda, Y. Nakahara: hep-lat/0208059
20. N. Ishii, H. Suganuma, H. Matsufuru: Phys. Rev. D **66**, 014507 (2002); Phys. Rev. D **66**, 094506 (2002)
21. K. Nomura, O. Miyamura, T. Umeda, H. Matsufuru: hep-lat/0209139; T. Umeda, H. Matsufuru, O. Miyamura, K. Nomura: hep-lat/0212007.
22. F. Karsch: Nucl. Phys. B **205**, 285 (1982)
23. J. Harada, A. S. Kronfeld, H. Matsufuru, N. Nakajima, T. Onogi: Phys. Rev. D **64**, 074501 (2001)
24. H. Matsufuru, T. Onogi, T. Umeda, Phys. Rev. D **64**, 114503 (2001)
25. G.P. Lepage, P.B. Mackenzie: Phys. Rev. D **48**, 2250 (1993)
26. G.P. Lepage: Nucl. Phys. B (Proc. Suppl.) **26**, 45 (1992); P.B. Mackenzie: ibid. **30**, 35 (1993); A.S. Kronkeld: ibid. **30**, 445 (1993)
27. T.R. Klassen: Nucl. Phys. B **533**, 557 (1998)
28. R. Sommer: Nucl. Phys. B **411**, 839 (1994)
29. J. Harada, H. Matsufuru, T. Onogi, A. Sugita: Phys. Rev. D **66**, 014509 (2002)
30. QCD-TARO Collaboration, S. Choe et al.: Nucl. Phys. B (Proc.Suppl.) **106**, 361 (2002); hep-lat/0307004
31. Particle Data Group Collaboration, D.E. Groom et al.: Eur. Phys. J. C **15** (2000) 1
32. The form of spectral function around a cutoff is also discussed in F. Karsch et al.: Phys. Rev. D **68** (2003) 014504
33. F. Karsch, M.T. Mehr, H. Satz: Z. Phys. C **37**, 617 (1988)
34. E. Eichten, K. Gottfried, T. Kinoshita, K.D. Lane, T.M. Yan, Phys. Rev. D **17**, 3090 (1978); **21**, 313(E) (1980); **21**, 203 (1980)
35. S. Digal, P. Petreczky, H. Satz: Phys. Rev. D **64**, 094015 (2001)